Iraqi Journal of Information and Communications Technology(IJICT)
Vol. 9, Issue 1, April 2026
www.ijict.edu.iq
ISSN:2222-758X
e-ISSN:2789-7362

CLASSIFICATION OF MRI BRAIN TUMOR IMAGES BASED ON MACHINE LEARNING ALGORITHM

Rana E. Azez[1], **Ayad A. Al-Ani**[2]
[1,2] Department of Information and Communication Engineering, College of Information Engineering, Al-Nahrain University, Jadriya, Baghdad, Iraq
rana.emad@coie-nahrain.edu.iq[1], ayad.a@nahrainuniv.edu.iq[2]
Corresponding Author: **Ayad A. Al-Ani**
Received:10/11/2024; Revised:19/02/2025; Accepted:14/11/2025
DOI:10.31987/ijict.9.1.306

***Abstract*- Brain Tumors (BTs) are serious medical conditions characterized by abnormal cellular growth in the brain. Magnetic Resonance Imaging (MRI) may be difficult and time-consuming for brain tumor identification and separation. This research automates the brain tumor classification, focusing on 4 diseases: gliomas, meningioma, and pituitary adenomas. Before employing Discrete Wavelet Transform (DWT) for tumor segmentation, MRI images should be converted to grayscale to improve speed and reduce computer complexity. PCA and Gray-Level Co-occurrence Matrix features are used to maximize feature extraction. The obtained features are classified using supervised K-Nearest Neighbours (KNN). The approach was tested using 2870 images, categorized as: 826 glioma, 822 meningioma, 827 pituitary adenoma, and 395 cancer-free images. The recommended approach used PCA and KNN to achieve 83% accuracy, however DWT and PCA together yielded 85% accuracy. The results show that the automated technique can quickly and accurately diagnose brain tumors.**

keywords: **MRI Brain Tumor, DWT, GLCM, PCA, KNN, Classification.**

I. INTRODUCTION

Healthcare providers must detect brain cancer early. Treatment outcomes improve with early brain tumor diagnosis. This understanding is essential for developing and accomplishing therapy goals since these illnesses may influence treatment and quality of life [1]. This improves illness treatment and early disease control, improving patient survival. Brain surgery is required to obtain biopsy samples for brain tumor identification and classification. Computational intelligence helps doctors classify brain cancers. Cancers of the brain and nervous system are deadly [2]. All human movements and behaviors are coordinated by brains. Brain structural variations are deadly and injure the body. This has led brain tumor diagnosis experts to create more advanced approaches. Most cancer doctors use Magnetic Resonance Imaging (MRI) and Computed Tomography (CT) scans to detect brain structure changes such size, shape, and placement, but they prefer MRI. Researchers and scientists are more interested in MRI. Clinicians are using indirect technologies like computer-aided brain medical picture processing to detect brain tumors. Multiple plant processing stages require segmentation and classification for medical imaging.

Creating a good classifier to distinguish abnormal and normal brain MRIs has been the focus [3],[4]. Feature extraction classifies brain MRI data. Another meaning of "feature extraction" is the design effort that converts an input image into one of less images to simplify computations on a restricted image collection Given the large amount of data in the input picture, feature extraction is a sad but necessary dimensional reduction method. Picture processing uses feature extraction to select important elements and remove extraneous ones. This feature visualization displays image data in low-dimensional space. Feature extraction removes extraneous information from a picture's distinctive features. Feature vectors depend on

image attributes [5],[6]. Understanding one definition in relation to another is possible. Image segmentation breaks up large brain MRI scans into smaller parts with similar features. Extracted features greatly influence segmentation features. Image intensity affects segmentation. Picture pixel intensity classification sets segmentation feature restrictions. Segmentation locates brain lesions [7],[8]. The researcher will then be advised of their tumor kind and possible tumors like glioma, meningioma, or pituitary gland if the brain is abnormal. This follows the training dataset.

The aim of this research is to enhance brain MRI categorization. This will assist in distinguishing brain tissues as normal or sick and appear how DWT affects accuracy. So, the main contributions of this work are as follows:

- A lightweight and efficient MRI brain tumor classification model using a combination of Discrete Wavelet Transform (DWT), Gray-Level Co-occurrence Matrix (GLCM), Principal Component Analysis (PCA), and K-Nearest Neighbors (KNN).
- Justification and evaluation of a 3-level DWT decomposition to extract rich texture features across multiple resolutions while minimizing computational cost.
- Extraction and analysis of five key GLCM texture features—contrast, correlation, entropy, homogeneity, and variance—and their role in balancing accuracy and complexity.
- Application of PCA to reduce the feature dimensionality, which improves processing efficiency and mitigates overfitting.
- Comparative evaluation of the model's performance with and without the DWT step, demonstrating the added value of wavelet-based texture enhancement.

II. Related Works

Brain tumor detection and classification have been widely explored using various image processing and machine learning techniques, particularly with MRI images due to their high contrast and detail of soft tissues. Numerous studies have proposed different preprocessing, feature extraction, and classification methods to improve accuracy and reduce computational cost.

In [9] applied deep learning architectures such as Inception-v3, VGG16, and ResNet-50 to classify brain tumors from MRI images. Their work demonstrated the high performance of Convolutional Neural Networks (CNNs) in automated tumor detection but required extensive computational resources and large datasets for effective training. In [10] investigated the use of the K-Nearest Neighbors (KNN) algorithm for brain tumor classification, where images were segmented using the Canny method and features were extracted using Hu Moments. Their approach achieved an average accuracy of 62% with 5-fold cross-validation, showing the feasibility of KNN but also highlighting the need for improved feature extraction to boost performance.

In [11] proposed a hybrid model combining CNN and Support Vector Machines (SVM) for tumor classification, along with threshold-based segmentation for detection. This combination aimed to leverage CNN's feature learning and SVM's classification robustness, achieving improved accuracy compared to single-model approaches.

Several other researchers have also explored advanced hybrid methods. In [12] developed an optimized system incorporating

ISSN:2222-758X
e-ISSN:2789-7362

preprocessing, segmentation, feature extraction, optimization, and detection. They used compound filters, threshold and histogram techniques, and GLCM for texture features, followed by an optimized CNN classifier for tumor detection.

Rasheed et al. [13] focused on improving MRI quality through anisotropic noise removal filtering, followed by segmentation using SVM. They localized tumors by classifying pixels based on brightness levels, which enhanced the precision of tumor localization in noisy MRI scans.

Susanto et al. [14] applied a single-level Discrete Wavelet Transform (DWT) for feature extraction, combining Gray-Level Co-occurrence Matrix (GLCM) and Local Binary Pattern (LBP) features. An SVM classifier was then used to differentiate between low-grade glioma (LGG) and high-grade glioma (HGG), demonstrating the effectiveness of wavelet-based texture features for tumor classification.

Despite these advancements, there is still a need for lightweight, interpretable, and computationally efficient methods that can achieve high accuracy without requiring large-scale computing infrastructure. While CNN and hybrid deep learning models have shown excellent performance, they often demand significant training resources and may not be practical in low-resource medical environments. This study addresses this gap by combining multi-level DWT, GLCM texture features, and PCA for dimensionality reduction with the KNN classifier, aiming to balance accuracy and complexity in brain tumor classification.

III. PROPOSED METHODOLOGY

In this section, present the proposed methodology designed for efficient and accurate brain tumor classification. The framework integrates multiple stages, starting from dataset preparation and preprocessing to feature extraction, dimensionality reduction, and final classification. The rationale behind this design is to combine the strengths of DWT for feature extraction, CA for reducing dimensionality, and GLCM for texture analysis, followed by KNN for classification. To demonstrate the contribution of DWT, developed two classification pipelines: one without DWT (i.e., see Fig. 1) and one with DWT (i.e., Fig. 2). Each step of the methodology is described in detail in the following subsections.

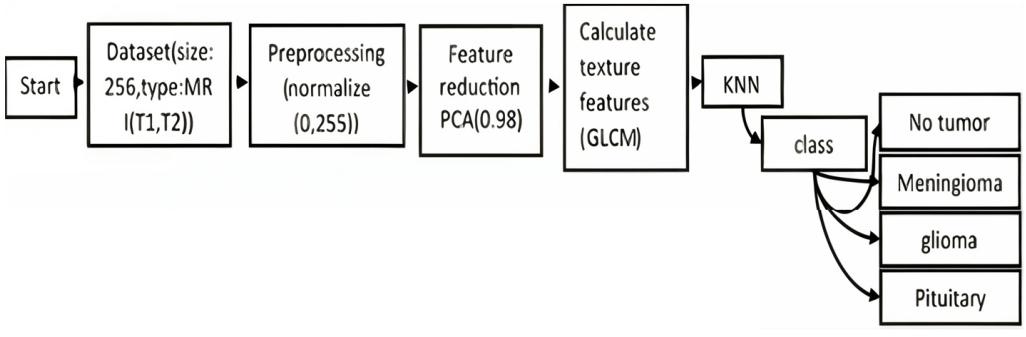

Figure 1: The proposed methodology without DWT.

ISSN:2222-758X
e-ISSN:2789-7362

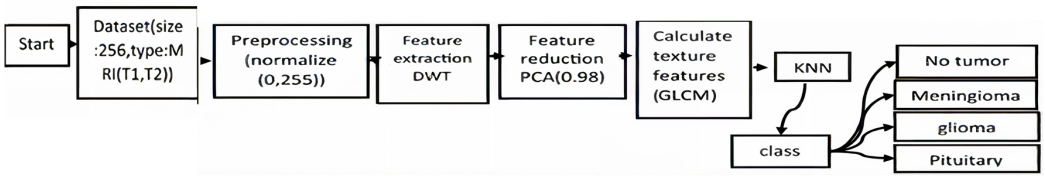

Figure 2: The proposed methodology with DWT.

A. *Dataset*

The dataset using in our research are installed from Kaggle website in 2020 [15]. Table I. show the category of the dataset appending to 3 types of brain tumors disease.

TABLE I
Dataset for MRI Brain Tumors.

Type of tumor	**No. of images for training**	**No. of images for testing**
Glioma	826	100
Meningioma	822	115
Pituitary	827	105
No- tumor	395	74
Total images	3870	394

B. *Pre-processing*

In this study, MRI brain tumor images underwent the following preprocessing steps before feature extraction as shown in Fig. 3 preprocessing includes resizing MRI images to 256×256 pixels and normalizing them to a single-channel grayscale format with intensity values from 0 to 255 which explain in detail:

1) **Image Resizing to 256×256 Pixels:** To ensure uniformity and reduce computational complexity, all input MRI images were resized to a fixed resolution of 256×256 pixels. This standardization allows the subsequent feature extraction and classification steps to operate on a consistent input size, ensuring fair comparison and reducing memory and processing requirements. Additionally, it enables efficient batch processing and integration with image processing algorithms that require fixed input dimensions [16].
2) **Conversion to Grayscale (Single-Channel):** Original MRI images, if in RGB format (3 channels), were converted to grayscale (1 channel). Since MRI images inherently carry structural and intensity-based information, color channels do not provide any additional value. Grayscale conversion simplifies the data, reduces dimensionality, and enhances the extraction of texture DWT (Discrete Wavelet Transform).
3) **Normalization (0 to 0.25 Range):** The pixel intensity values were normalized to a range of [0, 0.25]. This scaling ensures that all images are brought to a common intensity range, reducing the impact of lighting or scanner variability. Normalization also enhances numerical stability in subsequent feature extraction stages, particularly when calculating statistical or texture-based features. The choice of a small range (up to 0.25) helps in fine-grained texture distinction and avoids saturation during transformation or filtering operations.

ISSN:2222-758X
e-ISSN:2789-7362

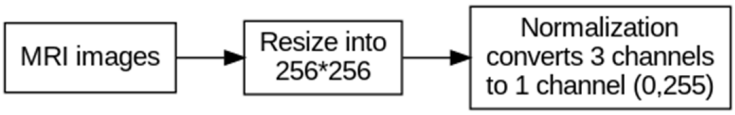

Figure 3: The steps of preprocessing.

C. Feature extraction by (DWT)

Achieving a higher level of accuracy in the classification stage requires the selection of an optimal set of features during the feature extraction stage. DWT is a highly effective mathematical tool that utilizes dyadic scales and positions to implement the wavelet transform [17]. This work employs the DWT technique for feature extraction from MRI brain images. DWT provides insights into both the time and frequency domains. Let us consider the square-integral function denoted as $x(t)$. The continuous wavelet transforms of $x(t)$ with respect to the specified wavelet $\Psi_{c,d}$ is defined in Eq. (1) as [17]:

$$W_{\Psi}(c,d) = \int_{-\infty}^{\infty} x(t)\ \Psi_{c,d}(t)\ dt \tag{1}$$

Then,

$$\Psi_{c,d}(t) = \frac{1}{\sqrt{c}}\,\Psi\left(\frac{t-c}{d}\right) \tag{2}$$

Where, $W_{\Psi}(c,d)$ is the wavelet coefficient, representing how much of the wavelet $\Psi(c,d)$ present in the signal $x(t)$ at scale 'c' and position 'd'. $x(t)$ is the input signal being analyzed. $\Psi(c,d)(t)$ is the scaled and translated version of the mother wavelet $\Psi(t)$. a is the scale parameter, controlling the width of the wavelet. d is the translation parameter, controlling the position of the wavelet along the time axis. t is the time; the independent variable of the signal. $1/\sqrt{c}$ represents the normalization factor, ensuring energy preservation during scaling. In $(t-c)/d$, the scaling (c) and translation (d) operation applied to the mother wavelet.

In Eq. (2), the variables 'c' and 'd' are defined as positive real numbers. The wavelet $\Psi_{c,d}(t)$ is derived from the mother wavelet $\Psi_{c,d}(t)$ through the application of translation and dilation, where 'c' denotes the dilation factor and 'd' indicates the translation parameter. The Haar wavelet is the most commonly utilized wavelet for image processing applications. To decompose an image into sub-bands with their corresponding DWT coefficients, two cascading low-pass and high-pass filters of the DWT technique are typically employed defined in the Eq. (3) and Eq. (4) as [17]:

$$ca_{j,k}(n) = DS\left[\sum_{n} x(n)\, g \times j(n-2^{j}k)\right] \tag{3}$$

$$cd_{j,k}(n) = DS\left[\sum_{n} x(n)\, h \times j(n-2^{j}k)\right] \tag{4}$$

Where, $ca_{(j,k)}(n)$ represents the approximation coefficients, representing the low-frequency components of the signal at scale j and position k. $cd_{(j,k)}(n)$ is the detail coefficients, representing the high-frequency components of the signal at scale j and position k. DS represents down-sampling operation, reducing the resolution of the coefficients to retain only

ISSN:2222-758X
e-ISSN:2789-7362

meaningful components. $x(n)$ is the discrete input signals. $g_j^{*(n)}$ is the low-pass filter derived from the scaling function associated with the wavelet. The filter captures low-frequency details. j is the scale index, corresponding to the resolution level of the decomposition. k is the translation index, representing the position of the coefficients within the scale. $h_j^{*(n)}$ is the high-pass filter derived from the wavelet function. The filter captures high-frequency details.

Typically, the DWT is employed for the single-level decomposition of an image in 2D, to meet specific constraints $Ca_{j,k}$ and Cd_j, k in Eq. (3) and Eq. (4) represent the approximation and detailed component coefficients, respectively, where the high and low pass filters are indicated by h(n) and g(n). The variables j and k represent the wavelet scale and transition factor, respectively, in the equations provided. In this study, a 3-level Haar DWT was applied to grayscale MRI images for feature extraction. Show the Fig. 4 that represent the level of DWT decomposes an image into four sub-bands (LL, LH, HL, HH) at each level, separating approximation and detail coefficients. The approximation component (LL) captures low-frequency information critical for preserving the structural features of medical images, while the detail coefficients capture high-frequency information such as edges and texture changes.

Selected 3-level decomposition as it offers a good trade-off between feature richness and computational efficiency. At this

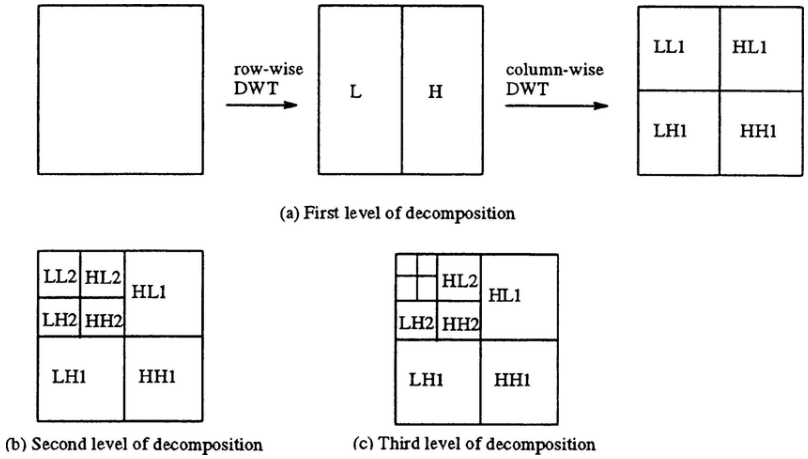

Figure 4: Level decomposition in DWT processing [17]

level, the image size is reduced from 256×256 to 32×32, enabling efficient processing while retaining essential texture information. Deeper decomposition (more than 3 levels) adds redundancy and computational overhead without significant gains in accuracy.

The Haar wavelet was chosen for its simplicity and fast computation, making it well-suited for real-time or resource-constrained applications. This step enhances the classifier's performance by simplifying the input data and highlighting tumor-relevant texture patterns essential for accurate classification.

D. Features Reducing

From the above techniques extract a vast number of characteristics. Therefore, the cclassification becomes more challenging as the number of characteristics grows. To reduce the complexity of categorization, feature reduction approaches

ISSN:2222-758X
e-ISSN:2789-7362

are employed. Feature reduction strategies remove redundant and associated characteristics, resulting in a smaller feature set. A comparative analysis of several dimensionality reduction strategies is provided in [18]. In research employs a Principal Component Analysis (PCA) feature reduction methodology. and use in this paper the PCA 0.98% from features extracted. PCA reduces dimensionality by computing and sorting the eigen vectors. Vectors having the highest covariance are discarded. In this study, the PCA was applied as a feature reduction technique following the extraction of GLCM features from multi-level DWT sub-bands. Due to the high-dimensional nature of the extracted texture features, removing PCA would significantly increase feature dimensionality, leading to longer training times, higher memory requirements, and a greater risk of overfitting. Additionally, PCA helps remove redundant and noisy features, which supports model generalization and enhances classification performance. Since the primary goal of our work is to develop a lightweight and efficient classification model suitable for resource-constrained environments (e.g., medical diagnostic tools with limited computing power), PCA was retained throughout all experiments. Therefore, we did not conduct a separate comparison with non-reduced features to avoid unnecessary computational burden and ensure the pipeline remains consistent and efficient.

E. Calculate texture features (GLCM)

The GLCM feature extraction technique is extensively employed to derive texture characteristics from a picture [19]. By examining the texture of the MRI picture, we may ascertain the information it contains, such as whether the brain is normal or exhibits an abnormal tumor. The GLCM feature extraction approach [19] is a straightforward yet dependable technique for deriving significant features from a picture. The GLCM is a two-dimensional histogram that measures the frequency of occurrence of the parameter in conjunction with the parameter. The GLCM technique assesses the frequency of occurrence of the and values at a designated distance and orientation. The angles employed in the GLCM algorithm for this investigation are 0, 45, and 90 degrees. Five features are retrieved from each corner property of the MRI image, resulting in a total of 25 features for one MRI picture. This study extracts properties such as contrast, correlation, energy, and homogeneity. Contrast is ascertained by analyzing the pixel intensity values of adjacent pixels within a picture. Contrasts are depicted using as shown in Eq. (5), where $f(x, y)$ denotes the coordinates of the picture pixels. Correlation is an image attribute characterized by the spatial dependency between two pixels. The correlation feature ranges from [-1,1] and as shown in Eq. (6), where represents the mean of the picture and σ is the standard deviation of the image, as shown in Eq.(6). Energy is defined as the frequency of identical pixel pairs, as shown in Eq. (7). Homogeneity quantifies the degree of local uniformity within a picture, as shown in Eq. (8). variance it is expectation of the squared deviation of a random variable x from its mean μ , as shown in Eq. (9). These features were chosen due to their proven ability to capture diverse and complementary aspects of image texture [19]:

$$\text{contrast} = \sum_{x=0}^{i=1} \sum_{y=0}^{j-1} (x-y)^2 f(x,y) \tag{5}$$

$$\text{correlation} = \frac{\sum_{x=0}^{i=1} \sum_{y=0}^{j-1} (x-y)^2 \, f(x,y) \, M_x M_y}{\sigma_x \sigma_y} \tag{6}$$

ISSN:2222-758X
e-ISSN:2789-7362

$$\text{Energy} = \sqrt{\sum_{x=0}^{i=1}\sum_{y=0}^{j-1} f^2(x,y)} \tag{7}$$

$$\text{Homogeneity} = \sum_{x=0}^{i=1}\sum_{y=0}^{j-1} \frac{1}{1+(x-y)^2}\, f(x,y) \tag{8}$$

$$\text{variance} = \frac{\sum(x-\mu)^2}{N} \tag{1}$$

Where the x and y indices the pixels in at image. M_x and M_y represents the means of the row and column. σ_x and σ_y represent the standard deviations of the row and column indices. $f(x,y)$ is the intensity value at the image (x,y),and the x is the intensity value of a pixel. μ represents the mean intensity of the image. The N is the total number of pixels.

F. Using KNN for training and classification

Using the obtained features, an image can be classified as either a glioma, meningioma, pituitary tumor, or showing no tumor at all. The proposed method makes use of the k-Nearest Neighbour algorithm for classification. The choice of KNN due to its simplicity, low training cost, and effectiveness when working with reduced features (after PCA). KNN is particularly suitable when the dataset is moderate in size and the features are well-structured (as is the case with DWT+GLCM). However, Interpretability and computational efficiency are important. The input's class is determined by looking at the classes of its k nearest neighbours; it is a supervised learning algorithm. This method is called a lazy algorithm because, unlike other supervised learning algorithms, it stores the training dataset instead of using it. Discover the nearest neighbours to an input by calculating the distances in the training dataset and selecting the first k examples with the least distance value. This is accomplished by making use of several distance measurement techniques. k is chosen because it is optimal. This approach makes use of the standard KNN algorithm. When calculating distance, traditional KNN algorithms [18] use tools like the Euclidean distance [18]. The class of the new input is then determined using the majority class of the nearest examples. To find the k closest neighbours, this method proposes using distance measurement techniques from the training dataset. Here is the formula for calculating the training-testing vectors' Euclidean distance [18].

$$d(a,b) = \sqrt{\sum_{i=1}^{n}(a_i - b_i)^2} \tag{10}$$

Where, a and b are point, and d is a distance between a and b.

IV. RESULT AND DISCUSSION

The proposed brain tumor classification algorithm is executed using the software Python on Visual Studio 2022 The experimentations are achieved on the system, Cpu : amd ryzen 7 5000, Gpu : NVIDIA GeForce RTX 3060 6GB and RAM : 16GB 5000HZ. The training and validation accuracy of the classifier is achieved 85% see the Fig. 5 presents the learning curve of the proposed KNN classifier. The training score (red line) remains consistently high across increasing training examples, indicating that the model fits the training data well. The cross-validation score (green line) shows a gradual

ISSN:2222-758X
e-ISSN:2789-7362

improvement as more training examples are added, suggesting that increasing the dataset size enhances generalization performance. The narrowing gap between training and cross-validation curves indicates reduced overfitting as the dataset grows. primary goal of this study was to develop a method for classifying MRI images into many groups that would best reflect normal brain, a normal brain tumors meningioma's, gliomas and pituitary.

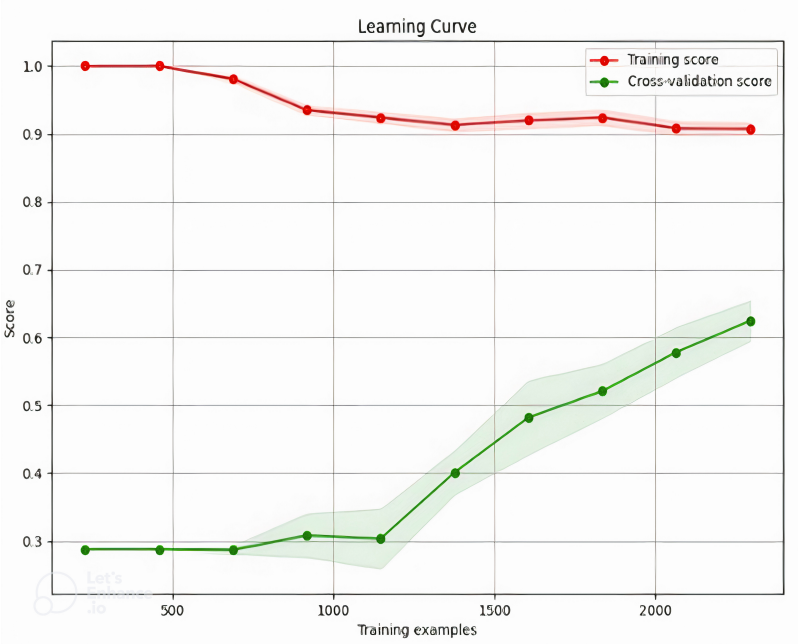

Figure 5: The training and validation accuracy of the classifier KNN.

A. *Performance Analysis*

Used precision, recall (sensitivity), average accuracy, and F1-score as performance measures to analyze the performance. These metrics were used to evaluate the performance. The F1-score is the performance indicator that is considered to be reliable in classification tasks. A confusion matrix illustrating the classification performance of the proposed model is presented in Fig. 6 Confusion matrix of the classification results at 83.5% accuracy. True labels are shown on the Y-axis and predicted labels on the X-axis. The matrix highlights the distribution of correctly and incorrectly classified MRI brain tumor images across four classes and Fig.7 Confusion matrix of classification outcomes at 85.5% accuracy. This matrix visualizes the number of correct and incorrect predictions across the four tumor classes, providing insight into the classifier's reliability. It demonstrates how well the model distinguishes between the four tumor types (Glioma, Meningioma, Pituitary, and No Tumor). Most predictions fall along the diagonal, indicating correct classification, while misclassifications appear in the off-diagonal elements. This visualization supports the reported accuracy of 85.5% and highlights areas where the model could be improved, particularly between Glioma and Meningioma. Each of the following mathematical expressions

ISSN:2222-758X
e-ISSN:2789-7362

may be used to indicate recall, precision, accuracy, and F1-score [20]:

$$\text{Accuracy} = \frac{TP + TN}{TN + TP + FP + FN} \tag{11}$$

$$\text{Precision} = \frac{TP}{FP + TP} \tag{12}$$

$$\text{Recall} = \frac{TP}{FN + TP} \tag{13}$$

$$\text{F1-score} = \frac{2 \times \text{Precision} \times \text{Recall}}{\text{Precision} \times \text{Recall}} \tag{14}$$

Where, $TP = True + ve$, and $FP = False + ve$, $FN = False - ve$, and $TN = True - ve$. To assess the model's

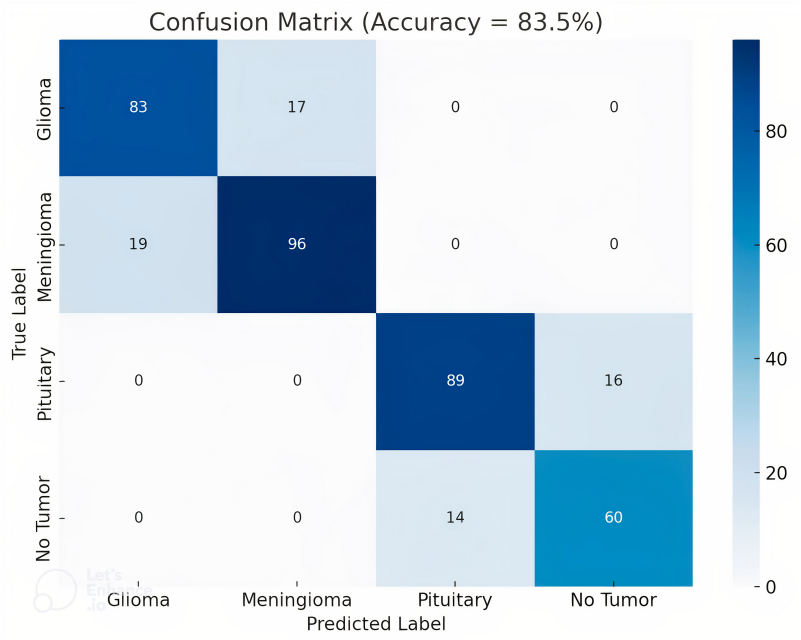

Figure 6: Confusion Matrix for 83.5% accuracy.

class-wise performance at an overall accuracy of 83.5%, present the confusion matrix in Fig.8 the matrix reveals high correct classification rates across most classes, particularly for Pituitary and No Tumor images. Some misclassifications are observed between Glioma and Meningioma, likely due to their overlapping textural features. Despite these errors, the model maintains strong diagnostic performance, validating the effectiveness of the extracted features and classification pipeline.

B. Discussion

At an improved accuracy of 85.5%, the confusion matrix in Fig.7 shows a noticeable reduction in misclassifications compared to the earlier result. Correct predictions for all classes increased, particularly for Glioma and Meningioma, indicating better generalization by the model. The reduction in confusion between tumor classes reflects the benefit of enhanced feature representation and dimensionality reduction. This improvement underscores the robustness of the proposed

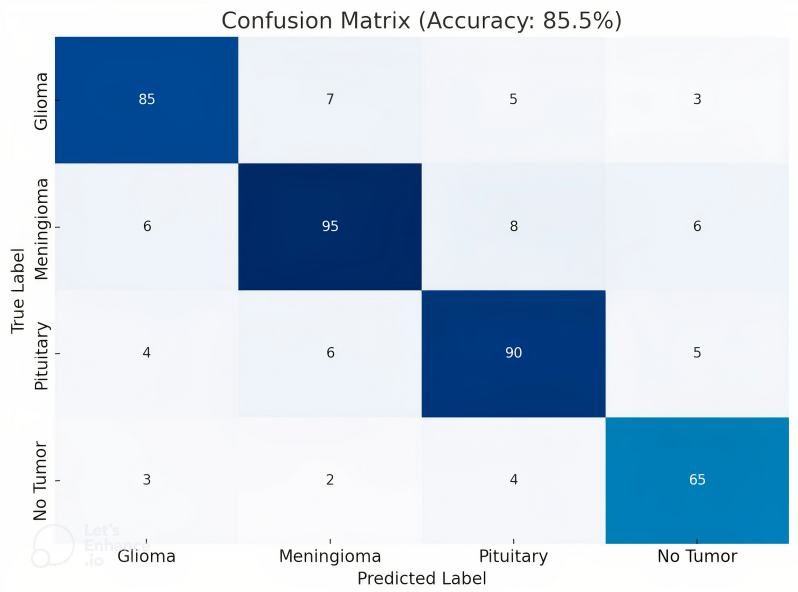

Figure 7: Confusion Matrix for 85.5% accuracy.

machine learning pipeline for MRI-based brain tumor classification. Comparing Figs. 6 and 7, the transition from 83.5% to 85.5% accuracy illustrates a meaningful enhancement in classification reliability, especially in reducing inter-class confusion between tumor types.

As for our choice of these features were extracted from the 3-level DWT subbands of each grayscale MRI image. Applying GLCM to each subband helps to capture multi-resolution texture characteristics, enhancing the descriptive power of the feature vector.

To reduce redundancy and dimensionality, Principal Component Analysis (PCA) was employed before feeding the features into the K-Nearest Neighbors (KNN) classifier. This combination strikes a balance between classification accuracy and computational efficiency, as it preserves the most informative features while minimizing unnecessary complexity. To see the difference well between with and without using DWT, look at the results Table II and Table III. Notice an increase in accuracy when using DWT. To evaluate the effectiveness of the proposed model, we compared the classification

TABLE II
The classification results of brain tumors Without DWT.

Type of tumor	Precision	Recall	F1-score	Accuracy
Glioma tumor	0.77	0.94	0.85	0.83%
Meningioma tumor	0.89	0.63	0.74	0.83%
Pituitary tumor	0.78	0.72	0.75	0.83%
No tumor	0.88	0.97	0.93	0.83%

performance with and without the application of DWT, and against existing related studies. While deep learning methods such as CNNs or hybrid models may offer slightly higher classification accuracy, they typically require significantly higher

TABLE III
The classification results of brain tumors With DWT.

Type of tumor	Precision	Recall	F1-score	Accuracy
Glioma tumor	0.82	0.91	0.86	0.85%
Meningioma tumor	0.84	0.67	0.74	0.85%
Pituitary tumor	0.86	0.85	0.85	0.85%
No tumor	0.87	0.97	0.92	0.85%

computational resources, larger training datasets, and longer training and inference times.

DWT-based approach achieves an accuracy of 85.5%, which is competitive when compared with similar machine learning techniques in the literature. Importantly, our method offers the advantage of being computationally lightweight and more suitable for real-time applications or deployment in resource-constrained environments such as edge devices or embedded systems.

The choice of using 3-level DWT allows for multi-resolution texture analysis without incurring the overhead of high-dimensional feature spaces. This balance between performance and complexity justifies the use of DWT in our model. Moreover, when compared to non-DWT feature extraction pipelines, our results demonstrate an improvement in texture detail preservation and overall classification accuracy. A summary of comparative accuracy with relevant prior studies is provided in Table IV accuracy score comparison between the proposed models and the sum of previous work.

TABLE IV
Accuracy score comparison between the proposed models and previous work.

Authors	Performance by Accuracy %
Mahmud et al. [9]	93.3
Khairandish et al., [10]	94.4
Oumarou, H., & Rismayanti, N.[11]	65.5
Proposed KNN	83.5
Proposed DWT+KNN	85.5

V. CONCLUSION

This paper presents an automated method for brain tumor classification that effectively distinguishes between normal and abnormal cases, focusing on glioma, meningioma, and pituitary adenoma. The proposed system integrates Discrete Wavelet Transform (DWT) for multi-resolution texture analysis, Principal Component Analysis (PCA) for dimensionality reduction, and Gray-Level Co-occurrence Matrix (GLCM) for texture feature extraction, with classification performed using the K-Nearest Neighbors (KNN) algorithm. This combination optimizes both image processing and classification efficiency. Tested on 2,870 MRI images, the method achieved an accuracy of 85%, confirming its ability to capture relevant tumor characteristics while maintaining low computational complexity. The integration of PCA demonstrated its role in reducing redundant features without sacrificing performance. These findings indicate that the approach is suitable for fast, accurate, and resource-efficient brain tumor diagnosis, which could be particularly valuable in clinical settings with limited computational infrastructure. Future work may focus on integrating this feature-based pipeline with hybrid or ensemble methods

to further improve accuracy while preserving simplicity.

FUNDING

None.

ACKNOWLEDGEMENT

The author would like to thank the reviewers for their valuable contribution in the publication of this paper.

CONFLICTS OF INTEREST

The author declares no conflict of interest.

REFERENCES

[1] A. Saleh, R. Sukaik, and S. S. Abu-Naser, "Brain tumor classification using deep learning," in 2020 International Conference on Assistive and Rehabilitation Technologies (iCareTech), IEEE, pp. 131–136, 2020.
[2] J. Kang, Z. Ullah, and J. Gwak, "MRI-based brain tumor classification using ensemble of deep features and machine learning classifiers," Sensors, vol. 21, no. 6, p. 2222, 2021.
[3] Viji and J. Jayaraj, "A Brain Abnormality Detection and Tissue Segmentation Technique by Using Dual Mode Classifier," International Arab Journal of Information Technology, vol. 13, no. 6, 2016.
[4] V. P. Rathi and S. Palani, "Brain Tumor MRI Image Classification with Feature Selection and Extraction using Linear Discriminant Analysis," CoRR, vol. abs/1208.2128, 2012.
[5] S. Bauer, R. Wiest, L.-P. Nolte, and M. Reyes, "A Survey of MRI-based Medical Image Analysis for Brain Tumor Studies," Physics in Medicine Biology, vol. 58, no. 13, pp. 1–44, 2011.
[6] E. Anjana and E. R. Kaur, "Review of Image Segmentation Technique," International Journal of Advanced Research in Computer Science, vol. 8, no. 4, pp. 36–39, 2017.
[7] S. Aruchamy, A. Haridasan, A. Verma, P. Bhattacharjee, S. N. Nandy, and S. R. K. Vadali, "Alzheimer's Disease Detection using Machine Learning Techniques in 3D MR Images," in 2020 National Conference on Emerging Trends on Sustainable Technology and Engineering Applications (NCETSTEA), IEEE, pp. 1–4, 2020.
[8] M. I. Mahmud, M. Mamun, and A. Abdelgawad, "A deep analysis of brain tumor detection from MR images using deep learning networks," Algorithms, vol. 16, no. 4, pp. 1–19, 2023.
[9] H. Oumarou and N. Rismayanti, "Automated Classification of Empon Plants: A Comparative Study Using Hu Moments and K-NN Algorithm," Indonesian Journal of Data and Science, vol. 4, no. 3, pp. 206–214, 2023.
[10] M. O. Khairandish, M. Sharma, V. Jain, J. M. Chatterjee, and N. Jhanjhi, "A hybrid CNN-SVM threshold segmentation approach for tumor detection and classification of MRI brain images," IRBM, vol. 43, no. 4, pp. 290–299, 2022.
[11] P. K. Ramtekkar, A. Pandey, and M. K. Pawar, "Accurate detection of brain tumor using optimized feature selection based on deep learning techniques," Multimedia Tools and Applications, vol. 82, no. 29, pp. 44623–44653, 2023.
[12] M. Rasheed, M. W. Iqbal, A. Jaffar, M. U. Ashraf, K. A. Almarhabi, A. M. Alghamdi, and A. A. Bahaddad, "Recognizing Brain Tumors Using Adaptive Noise Filtering and Statistical Features," Diagnostics, vol. 13, no. 8, p. 1451, 2023.
[13] A. Susanto, C. A. Sari, H. Rahmalan, and M. A. Doheir, "Support vector machine based discrete wavelet transform for magnetic resonance imaging brain tumor classification," TELKOMNIKA, vol. 21, no. 3, pp. 592–599, 2023.
[14] S. Bhuvaji, "Brain Tumor Classification (MRI) Dataset," Kaggle, 2020. [Online]. Available: https://www.kaggle.com/datasets/sartajbhuvaji/brain-tumor-classification-mri
[15] S. Shanjida, M. S. Islam, and M. Mohiuddin, "MRI-image based brain tumor detection and classification using CNN-KNN," in 2022 IEEE IAS Global Conference on Emerging Technologies (GlobConET), IEEE, pp. 900–905, 2022.
[16] A. Kumar, S. K. Pandey, N. Varshney, K. U. Singh, T. Singh, and M. A. Shah, "Distinctive approach in brain tumor detection and feature extraction using biologically inspired DWT method and SVM," Scientific Reports, vol. 13, no. 1, p. 22735, 2023.
[17] A. Warsun and A. T. Putra, "Diagnosis Using Brain Tumors Two-Dimensional Principal Component Analysis (2D-PCA) with K-nearest Neighbor (KNN) Classification Algorithm," Journal of Advances in Information Systems and Technology, vol. 3, no. 1, pp. 17–24, 2021.
[18] Y. Tarek, R. Elgohary, and M. Deif, "Brain tumor detection using GLCM and machine learning techniques," International Integrated Intelligent Systems, vol. 1, no. 2, 2024.
[19] M. Sandeep and A. Deepak, "Brain tumor detection using random forest algorithm in comparison with k-nearest neighbors algorithm to measure the accuracy, precision and recall," in AIP Conference Proceedings, vol. 2821, no. 1, p. 050027, AIP Publishing LLC, 2023.
[20] S. Ahmad and P. K. Choudhury, "On the Performance of Deep Transfer Learning Networks for Brain Tumor Detection Using MR Images," in IEEE Access, vol. 10, pp. 59099-59114, 2022, doi: 10.1109/ACCESS.2022.3179376.